FEBS openbio

FEBS PRESS science publishing by scientists

REVIEW

Novel aspects of the phosphorylation and structure of pathological tau: implications for tauopathy biomarkers

Taeko Kimura, Haruaki Sato, Maria Kano, Lisa Tatsumi and Taisuke Tomita

Laboratory of Neuropathology and Neuroscience, Graduate School of Pharmaceutical Sciences, The University of Tokyo, Japan

Keywords
Alzheimer's disease; blood biomarker; cryo-EM; phosphorylation; tau PET; tauopathy

Correspondence
T. Tomita, Laboratory of Neuropathology and Neuroscience, Graduate School of Pharmaceutical Sciences, The University of Tokyo, 7-3-1 Hongo, Bunkyo-Ku, Tokyo 113-0033, Japan
E-mail: taisuke@mol.f.u-tokyo.ac.jp

Taeko Kimura, Haruaki Sato, Maria Kano and Lisa Tatsumi contributed equally to this article

(Received 26 April 2023, revised 17 June 2023, accepted 29 June 2023)

doi:10.1002/2211-5463.13667

Edited by Koji Yamanaka

The deposition of highly phosphorylated and aggregated tau is a characteristic of tauopathies, including Alzheimer's disease. It has long been known that different isoforms of tau are aggregated in different cell types and brain regions in each tauopathy. Recent advances in analytical techniques revealed the details of the biochemical and structural biological differences of tau specific to each tauopathy. In this review, we explain recent advances in the analysis of post-translational modifications of tau, particularly phosphorylation, brought about by the development of mass-spectrometry and Phos-tag technology. We then discuss the structure of tau filaments in each tauopathy revealed by the advent of cryo-EM. Finally, we describe the progress in biofluid and imaging biomarkers for tauopathy. This review summarizes current efforts to elucidate the characteristics of pathological tau and the landscape of the use of tau as a biomarker to diagnose and determine the pathological stage of tauopathy.

Tau is a brain-specific microtubule (MT)-associated protein (MAP) first described by Weingarten *et al.* [1]. Tau is mainly localized in neuronal axons where it stabilizes axonal microtubules and then regulates axon outgrowth and axonal transport. These physiological functions of tau are regulated by phosphorylation with different protein kinases [2,3]. Tau is a heat-stable molecule consisting of 441 amino acids in the case of the longest human tau, consisting of three regions, an N-terminal projection domain and an MT-binding (MTB) domain, and C-terminal tail regions. Alternative mRNA splicing of the N-terminal insertions of exons 2 and 3 and the second MTB domain of exon 10 produces six isoforms, all of which are expressed in the

Abbreviations
AD, Alzheimer's disease; AGD, argyrophilic grain disease; Aβ, amyloid-β; CBD, corticobasal degeneration; Cdk5, cyclin-dependent kinase 5; CSF, cerebrospinal fluid; CTE, chronic traumatic encephalopathy; FBD, familial British dementia; FDD, familial Danish dementia; FTDP-17, frontotemporal dementia with parkinsonism-17; GGT, globular glial tauopathy; GSK3β, glycogen synthase kinase-3β; MAP, microtubule-associated protein; MT, microtubule; MTB, microtubule-binding; NFTs, neurofibrillary tangles; PART, primary age-related tauopathy; PHFs, paired helical filaments; PiD, Pick's disease; PP2A, protein phosphatase 2A; PSP, progressive supranuclear palsy; PTMs, post-translational modifications; SFs, straight filaments; SSPE, subacute sclerotic panencephalitis.

adult human brain. In particular, alternative splicing of exon 10 results in the generation of tau isoforms with either a three-repeat (3R) or four-repeat (4R) MTB domain [4]. 4R tau has stronger MT binding and assembly ability than 3R tau. Tau has attracted much attention since hyperphosphorylated tau (p-tau) was identified as a major component of neurofibrillary tangles (NFTs), a pathological hallmark of Alzheimer's disease (AD) [5–8]. While an amyloid-β (Aβ) deposition is linked to the pathological pathway of AD, there is also evidence that the frequency and distribution of NFTs are highly correlated with neuronal loss and progression of clinical symptoms [9,10]. In addition, the pathological role of tau has been intensively studied since the discovery of causative tau mutations in frontotemporal dementia with parkinsonism-17 (FTDP-17) in 1998. More than 40 mutations in the *MAPT* gene are now known [11,12]. There are many other neurodegenerative diseases in which deposits of hyperphosphorylated tau are found. These tau-involved diseases are collectively referred to as tauopathies and include AD, primary age-related tauopathy (PART), FTDP-17, corticobasal degeneration (CBD), progressive supranuclear palsy (PSP), Pick's disease (PiD), argyrophilic grain disease (AGD), globular glial tauopathy (GGT) and chronic traumatic encephalopathy (CTE) [13,14]. In addition to AD, tau deposits are found in the disease characterized by extracellular amyloid deposition; familial British dementia (FBD), familial Danish dementia (FDD), and prion disease. Interestingly, the aggregated tau in the brains of patients with tauopathies is highly phosphorylated in common, but there are known differences in the isoforms and cell types in which tau is deposited. Therefore, elucidating the differences in tau aggregates at the molecular level in each of these diseases will lead to understanding the pathogenic mechanism of each tauopathy.

Phosphorylation of tau deposited in the patients' brains

Biochemical analyses of the tau filaments obtained from the patients' brains revealed several post-translational modifications (PTMs), such as phosphorylation, ubiquitination, and acetylation. However, to date, phosphorylation is the most common PTM in deposited tau filaments and is utilized as pathological diagnostics of tauopathy.

Overview of tau phosphorylation

Tau phosphorylation is regulated by a balance between kinases [such as cyclin-dependent kinase 5 (Cdk5), glycogen synthase kinase-3β (GSK3β), and protein kinase A (PKA)] and phosphatases [such as protein phosphatase 2A (PP2A)] [15]. In postmortem brains of patients with tauopathies, this balance is disturbed, and tau is hyperphosphorylated. More than 50 tau phosphorylation sites have been reported in the brains of AD patients [3]. It has been suggested that phosphorylation of tau causes a conformational change in the protein and promotes the shedding of tau from microtubules by removing the positive charge of the MTB region [16]. Although it is controversial whether phosphorylation is a cause or a consequence of tau aggregation, the study of tau phosphorylation is key to understanding pathology. Since tau was identified as a component of NFT, many phosphorylation-specific antibodies against tau, such as AT8 (pS202/pT205) and PHF1 (pS396/pS404), have been used as markers of pathological tau. However, it has not been possible to estimate protein phosphorylation patterns or total phosphorylation levels although relative phosphorylation levels can be analyzed using p-tau antibodies. Here, we summarize the phosphorylation of tau in healthy and diseased brains, focusing on analysis by phosphate-binding tag (Phos-Tag) SDS/PAGE method and quantitative analysis by mass spectrometry (MS).

Phos-tag SDS/PAGE analysis of tau phosphorylation in cultured cells

Phos-tag SDS/PAGE allows distinguishing phosphorylated from nonphosphorylated tau by verifying the level of phosphorylation by the position of bands on the gel. Using this technique, the combination of phosphorylation sites (isotypes) and their level can be quantitatively estimated [17]. *In vitro* experiments revealed that normal tau has 12 different phosphorylation isotypes, with the major sites being T181, S202, T231, S235, and S404 (Fig. 1A) [18]. It was also found that phosphorylated tau in the combination of pS202, pT231, and pS235 was present at a high rate of 20.4% and that T231 was phosphorylated in approximately 50% of total tau molecules.

In the soluble fraction of the normal human brain, the three-repeat (3R) and four-repeat (4R) isoforms of tau without N-terminal inserts have low molecular weights and can be isolated from the phosphorylated bands, allowing analysis of their presence. Of the respective isoforms, 17.9% and 14.1% were unphosphorylated, suggesting that unphosphorylated tau is present to some extent. Detection of tau isolated by the Phos-tag method with the pS404 antibody showed that 57% of the total tau was phosphorylated.

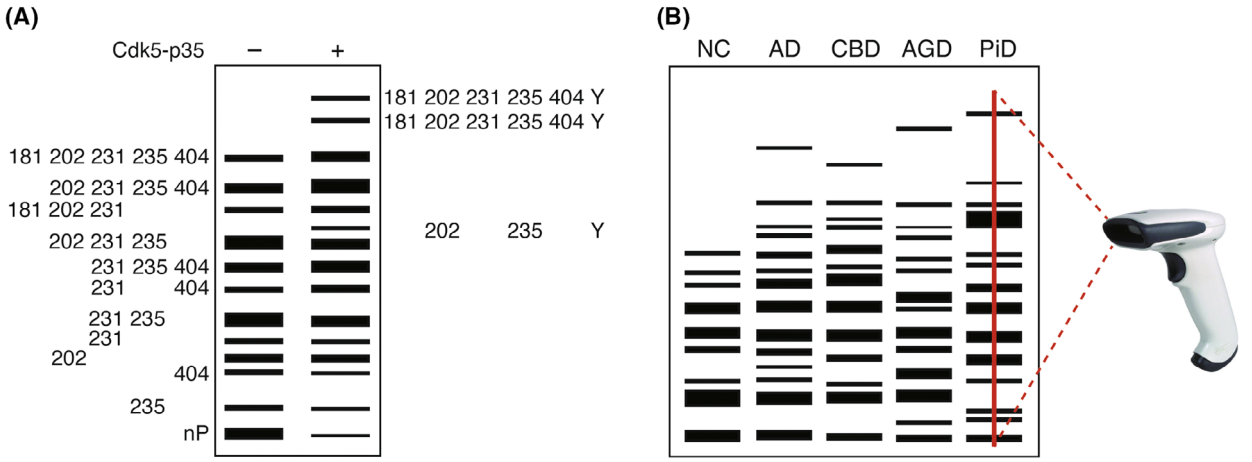

Fig. 1. Phos-tag SDS/PAGE analysis of tau phosphorylation. (A) Separation of phosphorylated tau by Cdk5-p35 in cultured cells using Phos-tag SDS/PAGE analysis. Numbers indicate the phosphorylated amino acid residues. nP means nonphosphorylated tau. Y represents unidentified phosphorylated site(s). (B) 'Phosphorylation barcode' of tau deposited in the different tauopathy brains. We propose that a simple diagnosis of tauopathy will be possible by reading banding patterns created by Phos-tag SDS/PAGE with a barcode reader.

Quantitative analysis experiments using MS with stable isotope labeled tau standards in the normal human brain were also performed and showed that more than 50% phosphorylation occurred for S404, similar to the Phos-Tag SDS/PAGE data [19]. Phos-Tag SDS/PAGE was then used to compare phosphorylation in AD, CBD, AGD, PSP, PiD, and other tauopathies. In the human brain, all six isoforms are expressed, and the banding pattern is complex. Therefore, a comparison was made using the banding pattern of Phos-tag SDS/PAGE. The results showed different banding patterns among tauopathies, suggesting the presence of disease-specific phosphorylation [18,20,21]. Immunoblotting with phosphorylated antibodies revealed differential site-specific phosphorylation in the temporal lobes of patients with different tauopathies. Increased pS202, pT231, and pS235 were observed in the AD brains, increased pS202 in the brains with PiD, and increased pS396 in the brains with AGD. In the future, the 'tau phosphorylation barcode', a phosphorylation-dependent banding pattern in Phos-tag SDS/PAGE shown by tau, is expected to be useful for understanding the pathogenesis and diagnosis of tauopathies (Fig. 1B).

Quantitative tau phosphorylation analysis among tauopathies using MS

A large study compared the frequency of tau phosphorylation in 49 AD patients with 42 healthy controls and found AD-specific phosphorylation at T217 and S262 [22]. In addition, phosphorylation can be compared quantitatively by determining the percentage of phosphorylated peptides among the total number of peptides containing each amino acid residue by MS. Phosphorylation sites that are more enriched in AD were found to be T111, S113, T153, T181, S199, S202, T205, T217, T231, S262, and S396 in the insoluble fraction compared with healthy control. And the effect of Aβ on tau PTM has also been studied, and T111, T153, and T217 were found as phosphorylation sites that are promoted with Aβ42 accumulation in the AD patient brains (Fig. 2) [19]. In a paper by Kametani *et al.* [23], phosphorylation analysis of insoluble tau revealed characteristic phosphorylation in each tauopathy. In AD, pS191 was as high as > 50%, whereas pS356 was barely detectable. In PiD, pS262 was absent. These could be related to the respective tau filament structures. In addition, T181, T217, T231, S235, S396, and S404 were highly phosphorylated at > 30% in all tauopathy patients (Fig. 2).

There are several challenges to tau phosphorylation studies in the human brain. One of them is postmortem time. In mice, dephosphorylation has been reported to occur at 1-min postmortem [24]. In human brains, tau is dephosphorylated during postmortem delay, even though aggregated tau is relatively resistant to dephosphorylation. Some studies have used biopsy samples from human brains, and a decrease in body temperature due to anesthesia during surgery also alters tau phosphorylation [25,26]. In other words, the exact phosphorylation state of tau in the human brain is not yet known. MS also analyzes proteins in fragments, making it difficult to identify tau isoforms. In

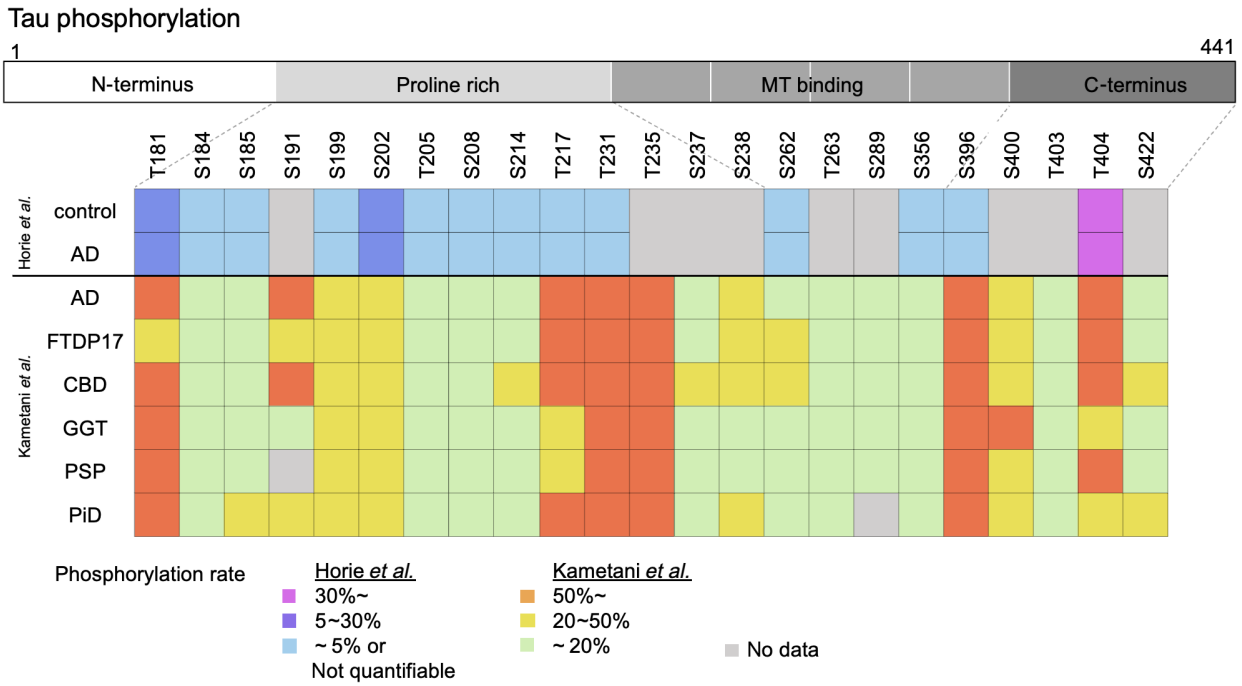

Fig. 2. Phosphorylation patterns of tau deposited in the tauopathy brains. The figure shows the phosphorylation sites of tau identified in each disease and the frequency (Horie *et al.* and Kametani *et al.* [19,23]).

addition, the relationship between tau PTMs and filament formation should be further discussed.

Structural analysis of tau filaments from the brain of tauopathy patients

Tau filaments have disease-specific morphologies, and their formation proceeds through the generation of disease-specific stable protofilament cores and the subsequent assembly of multiple cores. It is proposed that stable protofilament core structures determine tau filament structure, propagation, and neuropathic potential [27]. In recent years, remarkable advances in cryo-electron microscopy (cryo-EM) have established the structure-based classification of tauopathy (Fig. 3) [28,29].

AD fold

The formation of NFTs in AD begins in the locus coeruleus to the transentorhinal cortex and progressively affects the hippocampus, temporal cortex, and polymodal association areas [30]. There are two types of tau filaments, paired helical filaments (PHFs) and straight filaments (SFs), which are commonly found in AD [31,32]. They are composed of all six isoforms of 3R and 4R tau. Paired helical filaments are formed by two twisted, symmetrically coupled protofilaments, whereas SFs are asymmetrically coupled linear filaments. They share a common core structure with the same C-shaped core composed of residues G304-E380 (Fig. 3, AD), including repeat 3 (R3) and repeat 4 (R4) of the tau MTB domains, called AD fold [33,34]. The difference between PHFs and SFs structures lies in the contact surfaces of the two protofilaments: in PHFs, the paired helical structures are formed at the P332-Q336 interface; in SFs, the two protofilaments stack asymmetrically at the K317-S324 or P312-K321 interface. Furthermore, regardless of clinical or pathological progression, PHFs and SFs are remarkably identical in sporadic and inherited AD patients [35].

Further cryo-EM studies revealed the possible mechanism of the formation of AD fold tau filament. Primary age-related tauopathy is a neuropathological designation with features distinct from AD, and develops independently of Aβ plaques [34]. Notably, not only the biochemical character but also the structure of PART filaments was identical to that of AD. Furthermore, tau filaments with AD fold were identified in the brains of FBD, FDD, and prion disease [28,36]. These diseases are associated with the extracellular deposition of amyloids composed of distinct peptides: British amyloid, Danish amyloid, and prion proteins. Thus, these similarities suggest that the AD

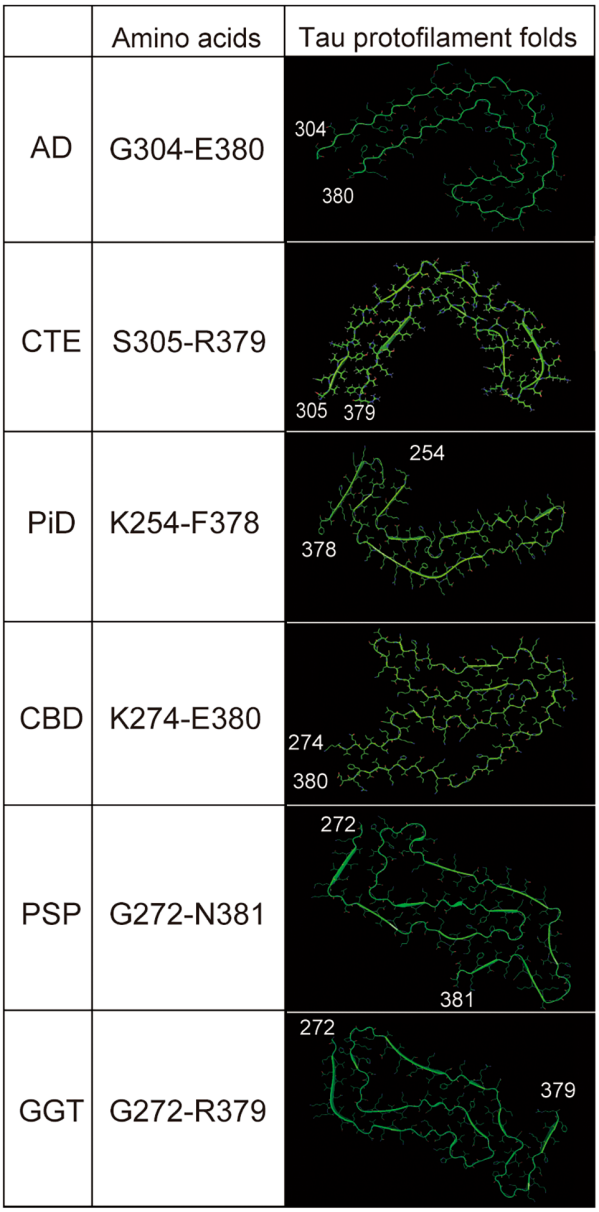

Fig. 3. Structures of the core of tau filaments revealed by cryo-EM analysis. Ribbon diagram of the cores of tau filaments. Numbers indicate amino acid residues in the 2N4R tau sequence. Each tau protofilament structure is visualized by PYMOL, Schrodinger, New York, NY,USA). Following EMDB datasets are used: AD, EMD-21207; CTE, EMD-14024; PiD, EMD-0077; CBD, EMD-10514; PSP, EMD-13218; GGT, EMD-13219. AD: PHFs and SFs share a C-shaped core composed of residues G304-E380. CTE: The cores of type I and II filaments are common structures like AD fold composed of S305-R379 consistent with SSPE. They are differ from AD by a hydrophobic cavity around E338-I354. PiD: NPFs and WPFs have a common J-shaped core consisting of K254-F378 of only 3R tau. CBD: Type I and II share the largest four-layered core like AGD core among tauopathies consisting of K274-E380. It contains a cavity surrounded by K290, K294 and K370. PSP: PSP cores have a three-layered folded structure consisting of residues G272-N381. Each repeat is systematically bent. Three additional density gaps are between N279 and G323, K294 and D314 and, K317, K321, and K340. GGT: GGT cores have three-layered structure like PSP fold composed of G272-R379.

fold of tau filaments was induced by age and extracellular amyloids.

CTE fold

In CTE, tau filaments are found in neurons and astrocytes around small blood vessels in the depths of cortical sulci [37,38]. Tau filaments are composed of all six isoforms, 3R and 4R, as in AD, and cryo-EM analysis revealed that CTE filaments have two types of helical filaments, 90% of which are type I: a helical filament [39]. The remaining 10% of filaments (type II) have a paired helical structure with a pronounced helical twist. They are analogous to the core of the AD fold. The cores are composed of K274-R379 of R3 and S305-R379 of R4. They differ from AD fold by a hydrophobic cavity around residues E338-I354 (Fig. 3, CTE). The presence of a cofactor in this cavity has been suggested, which could be some ions that leak from blood vessels due to injury damage. Recently, it has been suggested that sodium ions could be the most plausible cofactors, as discussed in detail in the next section [28,40].

Subacute sclerosing panencephalitis (SSPE) is a neurological disease following exposure to the measles virus and is described as a type of tauopathy that develops at a young age. Filamentous inclusions consist of 3R and 4R tau that accumulate in neurons and glial cells in the superficial cortex of the limbic system. Recent cryo-EM analysis revealed that the core structure of SSPE has a structure similar to that of CTE fold, with common protofilaments of the two types of filaments, type I accounting for more than 90% of the filaments observed and type II for less than 10%, similar to those observed in CTE (Fig. 3, CTE) [41]. As CTE and SSPE are chronic diseases, the inflammatory response might be involved in the formation of CTE fold.

PiD fold

Spherical tau filaments, called pick bodies, are seen in neurons in degenerative areas of the cortex in the

frontotemporal lobes of PiD patients. Filaments composed of a single 3R isoform [29,42]. Pick body-derived tau filaments are of two types, narrow and wide pick filaments (NPFs and WPFs). Narrow pick filaments (93%) are linear with twists, and WPFs (7%) are formed by two NPF protofilaments joined at their distal tips by van der Waals interactions. They share a common J-shaped protofilament core structure consisting of K254-F378 of 3R tau, including R1, R3, and R4. PiD is unique among tauopathies as only 3R tau aggregates and the structure is quite different from other tauopathies (Fig. 3, PiD). Thus, a 3R-specific disease-dependent mechanism would underlie the formation process of PiD fold [42].

CBD fold

The filaments are composed of only 4R tau observed not only in perivascular neurons, but astrocytes as astrocytic plaque in the cortex, brainstem, and basal ganglia [43]. They are observed in cell types similar to PSP. It accumulates in neurons at degenerative sites in the cortex. There are two types of helically twisted CBD tau filaments: narrow filaments (type I) and broad filaments (type II), paired inversely parallel to type I [44]. Type II is common in CBD patients. Both have in common that the core protofilaments are four-layered folded, consisting of K274-E380, the last residue of R1 R2, R3, the entire R4, and the 12 amino acids after R4. The CBD core is the largest among other tauopathies. The CBD core also contains a nonprotein-dense cavity. It is surrounded by side chains from K290 and K294 in R2 and K370 in R4 and has a positively charged hydrophilic space (Fig. 3, CBD). In the brains of CBD patients, filaments are particularly observed in perivascular astrocytes, suggesting that cofactors may enter the brain from the periphery [28].

Argyrophilic grain disease is late-onset dementia morphologically characterized by the presence of abundant spindle-shaped argyrophilic grains in neuronal processes and coiled bodies in oligodendrocytes. Biochemical studies revealed that AGD is a 4R tauopathy similar to PSP and CBD [29]. Intriguingly, the structure of tau filaments of AGD adopts a four-layered ordered structure that resembles CBD fold [28]. Also, other 4R tauopathies, such as aging-related tau astrogliopathy and FTDP-17 linked to *MAPT* intron-10 mutations +3 and +16, develop the tau filaments with CBD fold.

PSP fold

Tau aggregation and neuronal degeneration in PSP begin in neurons of the pallido-nigro-luysian axis and spread to the brainstem, basal ganglia, and cortex. Tau filaments are composed of 4R and accumulate in neurons, oligodendrocytes, and astrocytes as tufted astrocytes [43,45,46]. However, the structure of the tau filament in PSP was distinct from that of the CBD fold. PSP cores have a three-layered folded structure consisting of residues G272-N381 of 4R tau (Fig. 3, PSP) [28]. Each repeat is bent with a common sequence PGGG at the C-terminus, with R3 as the central layer and R2 and R4 storing R3. Three additional density gaps are observed. One is between N279 and G323, surrounded by hydrophobic side chains and possibly containing nonpolar molecules. The second is between K294 and D314 and is most likely a solvent molecule. The remaining one is located at the R3 and R4 interface, between positively charged K317, K321, and K340, and may correspond to an anion molecule. Notably, GGT, another 4R tauopathy, also develops tau filaments with PSP fold-like three-layered structure (Fig. 3, GGT), suggesting the similarities in the pathogenic process of these diseases [28].

Reconstitution of tau filaments

Tau is not an aggregation-prone protein. The N-terminal domain, including the positively charged proline-rich region, and the C-terminal domain inhibit the spontaneous assembly of full-length recombinant tau. Therefore, recombinant full-length tau assembly requires polyanionic assembly accelerators *in vitro*, such as heparin and dextran sulfate [47,48]. However, they have different structures from those in human patients, making it difficult to elucidate the molecular mechanisms underlying human tauopathies [49,50].

Based on cryo-EM studies above, it has become possible to reproduce patient filaments using 'cores'. Several amino acid sequences that induce AD-like filaments have been reported, including AD core sequences and portions of the proximal amino acids. Appropriate shaking and buffering conditions can produce tau filaments with PHF structures in the absence of cofactors [40,51,52]. The antibodies that recognize the recombinant AD tau core filaments recognize tau filaments in AD patients. This suggests that they may also share common structures. In addition, the cavities in CTE type II filaments may correspond to the sodium and chloride ions in the buffer. These ion levels are much lower than 200 mM in neurons, but damage-specific increases in concentration have been reported [40]. Nevertheless, these structural biology findings by cryo-EM facilitate the understanding of the pathogenic process of each tauopathy.

Biomarkers for tauopathy

Tauopathies have overlapping clinical symptoms and pathologic features [53]. Therefore, it is difficult to make an accurate diagnosis based on clinical symptoms or cognitive function tests. In addition, appropriate intervention methods differ according to the pathological progression of tauopathy. For example, the pathological process of AD follows many processes, from Aβ accumulation, which begins decades before the onset of the disease, to tau aggregation, neuronal death, and subsequent cognitive decline [54]. Therefore, there is an urgent need to discover effective biomarkers that can discriminate among diseases with similar symptoms and identify the specific pathological stage. Biochemical and structural differences in the aggregated tau would provide an opportunity to establish biomarkers that are specific to each of the tauopathies. Among the tauopathies, AD is the most extensively studied disease (Fig. 4) [55,56]. To date, amyloid PET and Aβ levels in cerebrospinal fluid (CSF), as well as plasma, are known biomarkers of Aβ accumulation in the brain [57,58]. For tau deposition, tau PET and tau levels in CSF, as well as plasma, have been extensively tested. Notably, phosphorylated and truncated forms of tau in biofluids have attracted attention because their increase occurs before tau aggregation and after Aβ accumulation, describing the more detailed pathological stage. In this section, we will discuss tau-based AD biomarkers and compare them to those in another tauopathy.

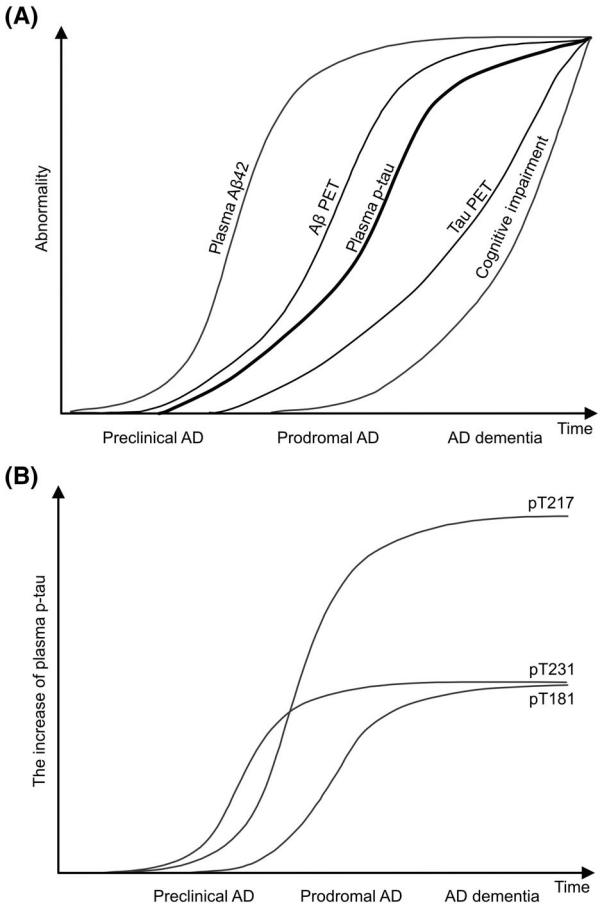

Fig. 4. Trajectory and biomarker changes of AD patients. (A) Schematic representation of pathological changes in the brain and plasma of AD patients. (B) Schematic representation of changes of phosphorylated tau in plasma of AD patients.

Biofluid biomarker

The levels of p-tau in CSF have been examined as a biomarker for AD and primary tauopathies including carriers with *MAPT* mutation [56,59,60], but CSF collection is invasive. Therefore, a method accurate and sensitive enough to detect p-tau in plasma, which is easier to collect but small in amount, has been searched for a decade. The modified MS technology has revealed a variety of p-tau species that correlate with AD pathology. And it has also shown that those p-tau species are N-terminal to midfragments and are different from the tau fragments that accumulate in the AD brain [61]. In addition, improved ELISA assays, such as Meso Scale Discovery (MSD) as well as single molecule array (Simoa) assays, allow the measurement of p-tau at concentrations as low as $fg{\cdot}mL^{-1}$ and have been used to validate the availability of these p-tau species [61–64].

pT181, pT217, and pT231 have been mainly investigated as biomarkers of AD [61,64–72]. All these p-tau species show high accuracy in discriminating between Aβ-positive and Aβ-negative patients even in the preclinical phase, high specificity for AD, and prognostic potential. Among them, pT181 is the most established species. Anti-Aβ treatment, such as Aducanumab, in AD patients reduced CSF pT181 [66], suggesting a causal relationship between increased plasma pT181 and Aβ accumulation since CSF pT181 levels correlate with plasma levels. pT217 is more sensitive than pT181 in specifically detecting Aβ-positive patients, and its increase in plasma occurs earlier than pT181, indicating a higher sensitivity to Aβ accumulation. In addition, the amount of pT231 in plasma increases earlier than pT217 or pT181, although no firm conclusions can be drawn about its accuracy. Importantly, the dynamic range of pT217 is generally greater than that of pT231 and pT181. Therefore, the measurement of multiple p-tau species together with Aβ in plasma is

important, and a composite biomarker would be required for accurate diagnosis of AD.

Other biomarkers such as pT205 [73], pS235 [74], brain-derived tau-specific isoforms [75], N-terminal tau [76–80], and midfragments of tau in CSF [81] are also expected to serve as AD biomarkers. Especially, MTBR domain fragments in CSF have recently been shown to potentially reflect tau accumulation in the AD brain [82] and may be elevated specifically in 4R tauopathy [59]. In contrast, total tau in plasma does not correlate with that in CSF, thus making it unsuitable as a biomarker [73]. The mechanism by which biomarkers change remains to be elucidated. Previous studies have shown that the amount of p-tau in CSF or plasma correlates with Aβ PET and tau PET, but Aβ PET shows more correlation [83–86]. We recently revealed that sAPPβ, which is a proteolytic fragment of amyloid precursor protein in the Aβ production pathway, positively regulates tau secretion in cultured cells [87]. As sAPPβ production is upregulated around Aβ plaques [88], this mechanism might be involved in the biological relationship between Aβ deposition and tau in biofluids.

Imaging biomarkers

Tau PET is a promising biomarker of tau aggregation because it can visualize tau aggregates in the brain while the patient is alive. The major first-generation tau PETs were developed in 2013, and one of them, [^{18}F]AV-1451 (Flortaucipir), was approved by the FDA as a biomarker of tau aggregation [89–91]. Subsequently, several second-generation tau PET tracers have been developed, such as [^{18}F]RO-948 and [^{18}F]MK-6420. In general, the reactivity of these tracers is limited to patients with AD and CTE, in which 3R and 4R mixed tau aggregates are deposited. It is consistent with the structural similarity of tau filaments of AD and CTE, as revealed by cryo-EM studies. In addition, [^{18}F]PI-2620 and [^{18}F]PM-PPB3/APN-1607 (Florzolotau) can bind to different tau aggregates independent of tau isoforms, such as those derived from primary tauopathies with only 4R tau aggregates. As the brain region with tau deposits differs from disease to disease, these tracers have the potential to discriminate tauopathies based on imaging data [92–97]. However, as recently shown in AD, the signal pattern shows heterogeneity even in the same disease using the same tracer [98]. Therefore, further imaging studies together with other tracers would be needed to achieve accurate diagnostics. Furthermore, recent structural analyses of tau filaments might also lead to the development of novel tracers targeting disease-specific tau aggregates. Based on the structure of tau filaments resolved by cryo-EM, the binding sites of [^{18}F]PM-PBB3 ligand to tau filaments were identified by cryo-EM analysis [34]. Also, simulation analyses suggested that the binding sites of the tracers to tau filaments from each type of tauopathy showed a unique pattern due to the difference in structure [99–104]. However, experimental structural analysis for these filaments and tracers is needed to confirm these putative binding sites. Nevertheless, modifying the tracer to bind to the specific structure of tau aggregates in each tauopathy is another solution for identifying the disease.

Concluding remarks and future prospectives

Recent progress in biochemical and structural analysis has shed light on the pathological properties of tau deposits in the brain. Plasma p-tau species and tau PET are promising biomarkers for tauopathy patients. Nevertheless, it is becoming apparent that these diseases are chronic, progressive conditions that require early diagnosis and intervention. Understanding the disease continuum and the relevance of biochemical and structural changes that contribute to abnormal tau metabolism, aggregation, deposition, and ultimately neurodegeneration is essential. Furthermore, the reasons why tau proteins with the same primary sequence undergo distinct folding, phosphorylation, and other modifications that are specifically observed in each tauopathy remain unclear. Therefore, it is critical to analyze the contribution of nonprotein components observed in cryo-EM structural analyses of tau filaments. Innovative approaches will be crucial in providing insight into the diagnosis and treatment of tauopathies, which account for a significant portion of neurodegenerative diseases.

Acknowledgements

The authors would like to thank our current and previous laboratory members for their helpful discussions. This work was supported in part by Nichiryo Co., Ltd., a Grant-in-Aid for Scientific Research (A) (19H01015, 23H00394 to TT) and (C) (23K06112 to TK) from the Japan Society for the Promotion of Science; Strategic Research Program for Brain Sciences from the Japan Agency for Medical Research and Development (JP22dm0207072, JP22dm0207073 to TT); Moonshot R&D from Japan Science and Technology Agency (JPMJMS2024 to TT). HS receives a research fellowship for young scientists (22J14955) from the Japan Society for the Promotion of Science.

LT receives Sadako O. Hirai Ban Award for Young Researchers. MK receives Nagai Memorial Research Scholarship from the Pharmaceutical Society of Japan.

Conflict of interest

The authors declare no conflict of interest.

Author contributions

TK, HS, LT, and MK wrote the draft and revised it. TT was involved in discussing, drafting, and editing the manuscript. All authors approved the submitted version.

References

1 Weingarten MD, Lockwood AH, Hwo SY and Kirschner MW (1975) A protein factor essential for microtubule assembly. *Proc Natl Acad Sci USA* **72**, 1858–1862.
2 Iqbal K, Liu F and Gong CX (2016) Tau and neurodegenerative disease: the story so far. *Nat Rev Neurol* **12**, 15–27.
3 Wegmann S, Biernat J and Mandelkow E (2021) A current view on tau protein phosphorylation in Alzheimer's disease. *Curr Opin Neurobiol* **69**, 131–138.
4 Goedert M, Spillantini MG, Potier MC, Ulrich J and Crowther RA (1989) Cloning and sequencing of the cDNA encoding an isoform of microtubule-associated protein tau containing four tandem repeats: differential expression of tau protein mRNAs in human brain. *EMBO J* **8**, 393–399.
5 Ihara Y, Nukina N, Miura R and Ogawara M (1986) Phosphorylated tau protein is integrated into paired helical filaments in Alzheimer's disease. *J Biochem* **99**, 1807–1810.
6 Kosik KS, Joachim CL and Selkoe DJ (1986) Microtubule-associated protein tau (tau) is a major antigenic component of paired helical filaments in Alzheimer disease. *Proc Natl Acad Sci USA* **83**, 4044–4048.
7 Nukina N, Kosik KS and Selkoe DJ (1987) Recognition of Alzheimer paired helical filaments by monoclonal neurofilament antibodies is due to crossreaction with tau protein. *Proc Natl Acad Sci USA* **84**, 3415–3419.
8 Lee VMY, Balin BJ, Otvos L and Trojanowski JQ (1991) A68: a major subunit of paired helical filaments and derivatized forms of normal tau. *Science* **251**, 675–678.
9 Knopman DS, Amieva H, Petersen RC, Chételat G, Holtzman DM, Hyman BT, Nixon RA and Jones DT (2021) Alzheimer disease. *Nat Rev Dis Primers* **7**, 33.
10 Gómez-Isla T, Hollister R, West H, Mui S, Growdon JH, Petersen RC, Parisi JE and Hyman BT (1997) Neuronal loss correlates with but exceeds neurofibrillary tangles in Alzheimer's disease. *Ann Neurol* **41**, 17–24.
11 Mann DMA and Snowden JS (2017) Frontotemporal lobar degeneration: pathogenesis, pathology and pathways to phenotype. *Brain Pathol* **27**, 723–736.
12 Strang KH, Golde TE and Giasson BI (2019) MAPT mutations, tauopathy, and mechanisms of neurodegeneration. *Lab Invest* **99**, 912–928.
13 Kovacs GG, Ghetti B and Goedert M (2022) Classification of diseases with accumulation of tau protein. *Neuropathol Appl Neurobiol* **48**, e12792.
14 Stamelou M, Respondek G, Giagkou N, Whitwell JL, Kovacs GG and Höglinger GU (2021) Evolving concepts in progressive supranuclear palsy and other 4-repeat tauopathies. *Nat Rev Neurol* **17**, 601–620.
15 Wang Y and Mandelkow E (2016) Tau in physiology and pathology. *Nat Rev Neurosci* **17**, 5–21.
16 Johnson GVW and Stoothoff WH (2004) Tau phosphorylation in neuronal cell function and dysfunction. *J Cell Sci* **117**, 5721–5729.
17 Kimura T, Sharma G, Ishiguro K and Hisanaga S-I (2018) Phospho-tau Bar code: analysis of phosphoisotypes of tau and its application to tauopathy. *Front Neurosci* **12**, 44.
18 Kimura T, Hosokawa T, Taoka M, Tsutsumi K, Ando K, Ishiguro K, Hosokawa M, Hasegawa M and Hisanaga SI (2016) Quantitative and combinatory determination of in situ phosphorylation of tau and its FTDP-17 mutants. *Sci Rep* **6**, 33479.
19 Horie K, Barthélemy NR, Mallipeddi N, Li Y, Franklin EE, Perrin RJ, Bateman RJ and Sato C (2020) Regional correlation of biochemical measures of amyloid and tau phosphorylation in the brain. *Acta Neuropathol Commun* **8**, 149.
20 Samimi N, Sharma G, Kimura T, Matsubara T, Huo A, Chiba K, Saito Y, Murayama S, Akatsu H, Hashizume Y *et al.* (2021) Distinct phosphorylation profiles of tau in brains of patients with different tauopathies. *Neurobiol Aging* **108**, 72–79.
21 Kimura T, Hatsuta H, Masuda-Suzukake M, Hosokawa M, Ishiguro K, Akiyama H, Murayama S, Hasegawa M and Hisanaga SI (2016) The abundance of nonphosphorylated tau in mouse and human tauopathy brains revealed by the use of phos-tag method. *Am J Pathol* **186**, 398–409.
22 Wesseling H, Mair W, Kumar M, Schlaffner CN, Tang S, Beerepoot P, Fatou B, Guise AJ, Cheng L, Takeda S *et al.* (2020) Tau PTM profiles identify patient heterogeneity and stages of Alzheimer's disease. *Cell* **183**, 1699–1713.e13.
23 Kametani F, Yoshida M, Matsubara T, Murayama S, Saito Y, Kawakami I, Onaya M, Tanaka H, Kakita

A, Robinson AC *et al.* (2020) Comparison of common and disease-specific post-translational modifications of pathological tau associated with a wide range of tauopathies. *Front Neurosci* **14**, 581936.
24 Wang Y, Zhang Y, Hu W, Xie S, Gong CX, Iqbal K and Liu F (2015) Rapid alteration of protein phosphorylation during postmortem: implication in the study of protein phosphorylation. *Sci Rep* **5**, 15709.
25 Matsuo ES, Shin RW, Billingsley ML, Van de Voorde A, O'Connor M, Trojanowski JQ and Lee VMY (1994) Biopsy-derived adult human brain tau is phosphorylated at many of the same sites as Alzheimer's disease paired helical filament tau. *Neuron* **13**, 989–1002.
26 Whittington RA, Bretteville A, Dickler MF and Planel E (2013) Anesthesia and tau pathology. *Prog Neuropsychopharmacol Biol Psychiatry* **47**, 147–155.
27 Arima K (2006) Ultrastructural characteristics of tau filaments in tauopathies: immuno-electron microscopic demonstration of tau filaments in tauopathies. *Neuropathology* **26**, 475–483.
28 Shi Y, Zhang W, Yang Y, Murzin AG, Falcon B, Kotecha A, van Beers M, Tarutani A, Kametani F, Garringer HJ *et al.* (2021) Structure-based classification of tauopathies. *Nature* **598**, 359–363.
29 Tarutani A, Adachi T, Akatsu H, Hashizume Y, Hasegawa K, Saito Y, Robinson AC, Mann DMA, Yoshida M, Murayama S *et al.* (2022) Ultrastructural and biochemical classification of pathogenic tau, α-synuclein and TDP-43. *Acta Neuropathol* **143**, 613–640.
30 Braak H and Braak E (1991) Neuropathological stageing of Alzheimer-related changes. *Acta Neuropathol* **82**, 239–259.
31 Goedert M, Eisenberg DS and Crowther RA (2017) Propagation of tau aggregates and neurodegeneration. *Annu Rev Neurosci* **40**, 189–210.
32 Goedert M (2018) Tau filaments in neurodegenerative diseases. *FEBS Lett* **592**, 2383–2391.
33 Fitzpatrick AWP, Falcon B, He S, Murzin AG, Murshudov G, Garringer HJ, Crowther RA, Ghetti B, Goedert M and Scheres SHW (2017) Cryo-EM structures of tau filaments from Alzheimer's disease. *Nature* **547**, 185–190.
34 Shi Y, Murzin AG, Falcon B, Epstein A, Machin J, Tempest P, Newell KL, Vidal R, Garringer HJ, Sahara N *et al.* (2021) Cryo-EM structures of tau filaments from Alzheimer's disease with PET ligand APN-1607. *Acta Neuropathol* **141**, 697–708.
35 Falcon B, Zhang W, Schweighauser M, Murzin AG, Vidal R, Garringer HJ, Ghetti B, Scheres SHW and Goedert M (2018) Tau filaments from multiple cases of sporadic and inherited Alzheimer's disease adopt a common fold. *Acta Neuropathol* **136**, 699–708.
36 Hallinan GI, Hoq MR, Ghosh M, Vago FS, Fernandez A, Garringer HJ, Vidal R, Jiang W and Ghetti B (2021) Structure of tau filaments in prion protein amyloidoses. *Acta Neuropathol* **142**, 227–241.
37 McKee AC, Cairns NJ, Dickson DW, Folkerth RD, Dirk Keene C, Litvan I, Perl DP, Stein TD, Vonsattel JP, Stewart W *et al.* (2016) The first NINDS/NIBIB consensus meeting to define neuropathological criteria for the diagnosis of chronic traumatic encephalopathy. *Acta Neuropathol* **131**, 75–86.
38 Arena JD, Smith DH, Lee EB, Gibbons GS, Irwin DJ, Robinson JL, Lee VMY, Trojanowski JQ, Stewart W and Johnson VE (2020) Tau immunophenotypes in chronic traumatic encephalopathy recapitulate those of ageing and Alzheimer's disease. *Brain* **143**, 1572–1587.
39 Falcon B, Zivanov J, Zhang W, Murzin AG, Garringer HJ, Vidal R, Crowther RA, Newell KL, Ghetti B, Goedert M *et al.* (2019) Novel tau filament fold in chronic traumatic encephalopathy encloses hydrophobic molecules. *Nature* **568**, 420–423.
40 Lövestam S, Koh FA, van Knippenberg B, Kotecha A, Murzin AG, Goedert M and Scheres SHW (2022) Assembly of recombinant tau into filaments identical to those of Alzheimer's disease and chronic traumatic encephalopathy. *Elife* **11**, e76494.
41 Qi C, Hasegawa M, Takao M, Sakai M, Sasaki M, Mizutani M, Akagi A, Iwasaki Y, Miyahara H, Yoshida M *et al.* (2023) Identical tau filaments in subacute sclerosing panencephalitis and chronic traumatic encephalopathy. *Acta Neuropathol Commun* **11**, 74.
42 Falcon B, Zhang W, Murzin AG, Murshudov G, Garringer HJ, Vidal R, Crowther RA, Ghetti B, Scheres SHW and Goedert M (2018) Structures of filaments from Pick's disease reveal a novel tau protein fold. *Nature* **561**, 137–140.
43 Komori T, Arai N, Oda M, Nakayama H, Mori H, Yagishita S, Takahashi T, Amano N, Murayama S, Murakami S *et al.* (1998) Astrocytic plaques and tufts of abnormal fibers do not coexist in corticobasal degeneration and progressive supranuclear palsy. *Acta Neuropathol* **96**, 401–408.
44 Zhang W, Tarutani A, Newell KL, Murzin AG, Matsubara T, Falcon B, Vidal R, Garringer HJ, Shi Y, Ikeuchi T *et al.* (2020) Novel tau filament fold in corticobasal degeneration. *Nature* **580**, 283–287.
45 Komori T, Shibata N, Kobayashi M, Sasaki S and Iwata M (1998) Inducible nitric oxide synthase (iNOS)-like immunoreactivity in argyrophilic, tau-positive astrocytes in progressive supranuclear palsy. *Acta Neuropathol* **95**, 338–344.
46 Kovacs GG (2020) Astroglia and tau: new perspectives. *Front Aging Neurosci* **12**, 96.
47 Goedert M, Jakes R, Spillantini MG, Hasegawa M, Smith MJ and Crowther RA (1996) Assembly of microtubule-associated protein tau into Alzheimer-like

filaments induced by sulphated glycosaminoglycans. *Nature* **383**, 550–553.
48 Masuda-Suzukake M, Suzuki G, Hosokawa M, Nonaka T, Goedert M and Hasegawa M (2020) Dextran sulphate-induced tau assemblies cause endogenous tau aggregation and propagation in wild-type mice. *Brain Commun* **2**, fcaa091.
49 Guo JL, Narasimhan S, Changolkar L, He Z, Stieber A, Zhang B, Gathagan RJ, Iba M, McBride JD, Trojanowski JQ *et al.* (2016) Unique pathological tau conformers from Alzheimer's brains transmit tau pathology in nontransgenic mice. *J Exp Med* **213**, 2635–2654.
50 Zhang W, Falcon B, Murzin AG, Fan J, Crowther RA, Goedert M and Scheres SHW (2019) Heparin-induced tau filaments are polymorphic and differ from those in alzheimer's and pick's diseases. *Elife* **8**, e43584.
51 Carlomagno Y, Manne S, DeTure M, Prudencio M, Zhang YJ, Hanna Al-Shaikh R, Dunmore JA, Daughrity LM, Song Y, Castanedes-Casey M *et al.* (2021) The AD tau core spontaneously self-assembles and recruits full-length tau to filaments. *Cell Rep* **34**, 108843.
52 Li X, Zhang S, Liu Z, Tao Y, Xia W, Sun Y, Liu C, Le W, Sun B and Li D (2022) Subtle change of fibrillation condition leads to substantial alteration of recombinant tau fibril structure. *iScience* **25**, 105645.
53 Zhang Y, Wu KM, Yang L, Dong Q and Yu JT (2022) Tauopathies: new perspectives and challenges. *Mol Neurodegener* **171**, 1–29.
54 Mattsson-Carlgren N, Andersson E, Janelidze S, Ossenkoppele R, Insel P, Strandberg O, Zetterberg H, Rosen HJ, Rabinovici G, Chai X *et al.* (2020) Aβ deposition is associated with increases in soluble and phosphorylated tau that precede a positive tau PET in Alzheimer's disease. *Sci Adv* **6**, eaaz2387.
55 Zetterberg H and Blennow K (2021) Moving fluid biomarkers for Alzheimer's disease from research tools to routine clinical diagnostics. *Mol Neurodegener* **16**, 10.
56 Simrén J, Elmgren A, Blennow K and Zetterberg H (2023) Fluid biomarkers in Alzheimer's disease. *Adv Clin Chem* **112**, 249–281.
57 Kaneko N, Nakamura A, Washimi Y, Kato T, Sakurai T, Arahata Y, Bundo M, Takeda A, Niida S, Ito K *et al.* (2014) Novel plasma biomarker surrogating cerebral amyloid deposition. *Proc Jpn Acad Ser B Phys Biol Sci* **90**, 353–364.
58 Brand AL, Lawler PE, Bollinger JG, Li Y, Schindler SE, Li M, Lopez S, Ovod V, Nakamura A, Shaw LM *et al.* (2022) The performance of plasma amyloid beta measurements in identifying amyloid plaques in Alzheimer's disease: a literature review. *Alzheimers Res Ther* **14**, 195.
59 Horie K, Barthélemy NR, Spina S, VandeVrede L, He Y, Paterson RW, Wright BA, Day GS, Davis AA, Karch CM *et al.* (2022) CSF tau microtubule-binding region identifies pathological changes in primary tauopathies. *Nat Med* **28**, 2547–2554.
60 Sato C, Mallipeddi N, Ghoshal N, Wright BA, Day GS, Davis AA, Kim AH, Zipfel GJ, Bateman RJ, Gabelle A *et al.* (2021) MAPT R406W increases tau T217 phosphorylation in absence of amyloid pathology. *Ann Clin Transl Neurol* **8**, 1817–1830.
61 Karikari TK, Ashton NJ, Brinkmalm G, Brum WS, Benedet AL, Montoliu-Gaya L, Lantero-Rodriguez J, Pascoal TA, Suárez-Calvet M, Rosa-Neto P *et al.* (2022) Blood phospho-tau in Alzheimer disease: analysis, interpretation, and clinical utility. *Nat Rev Neurol* **18**, 400–418.
62 Mielke MM, Hagen CE, Xu J, Chai X, Vemuri P, Lowe VJ, Airey DC, Knopman DS, Roberts RO, Machulda MM *et al.* (2018) Plasma phospho-tau181 increases with Alzheimer's disease clinical severity and is associated with tau- and amyloid-positron emission tomography. *Alzheimers Dement* **14**, 989–997.
63 Tatebe H, Kasai T, Ohmichi T, Kishi Y, Kakeya T, Waragai M, Kondo M, Allsop D and Tokuda T (2017) Quantification of plasma phosphorylated tau to use as a biomarker for brain Alzheimer pathology: pilot case-control studies including patients with Alzheimer's disease and down syndrome. *Mol Neurodegener* **12**, 63.
64 Janelidze S, Bali D, Ashton NJ, Barthélemy NR, Vanbrabant J, Stoops E, Vanmechelen E, He Y, Dolado AO, Triana-Baltzer G *et al.* (2022) Head-to-head comparison of 10 plasma phospho-tau assays in prodromal Alzheimer's disease. *Brain* **146**, 1592–1601.
65 Gonzalez-Ortiz F, Kac PR, Brum WS, Zetterberg H, Blennow K and Karikari TK (2023) Plasma phospho-tau in Alzheimer's disease: towards diagnostic and therapeutic trial applications. *Mol Neurodegener* **18**, 18.
66 Avgerinos KI, Ferrucci L and Kapogiannis D (2021) Effects of monoclonal antibodies against amyloid-β on clinical and biomarker outcomes and adverse event risks: a systematic review and meta-analysis of phase III RCTs in Alzheimer's disease. *Ageing Res Rev* **68**, 101339.
67 Thijssen EH, La Joie R, Wolf A, Strom A, Wang P, Iaccarino L, Bourakova V, Cobigo Y, Heuer H, Spina S *et al.* (2020) Diagnostic value of plasma phosphorylated tau181 in Alzheimer's disease and frontotemporal lobar degeneration. *Nat Med* **26**, 387–397.
68 Ashton NJ, Hye A, Rajkumar AP, Leuzy A, Snowden S, Suárez-Calvet M, Karikari TK, Schöll M, La Joie R, Rabinovici GD *et al.* (2020) An update on blood-based biomarkers for non-Alzheimer

neurodegenerative disorders. *Nat Rev Neurol* **16**, 265–284.
69 Milà-Alomà M, Ashton NJ, Shekari M, Salvadó G, Ortiz-Romero P, Montoliu-Gaya L, Benedet AL, Karikari TK, Lantero-Rodriguez J, Vanmechelen E *et al.* (2022) Plasma p-tau231 and p-tau217 as state markers of amyloid-β pathology in preclinical Alzheimer's disease. *Nat Med* **28**, 1797–1801.
70 Bayoumy S, Verberk IMW, den Dulk B, Hussainali Z, Zwan M, van der Flier WM, Ashton NJ, Zetterberg H, Blennow K, Vanbrabant J *et al.* (2021) Clinical and analytical comparison of six Simoa assays for plasma P-tau isoforms P-tau181, P-tau217, and P-tau231. *Alzheimers Res Ther* **13**, 198.
71 Ashton NJ, Puig-Pijoan A, Milà-Alomà M, Fernández-Lebrero A, García-Escobar G, González-Ortiz F, Kac PR, Brum WS, Benedet AL, Lantero-Rodriguez J *et al.* (2022) Plasma and CSF biomarkers in a memory clinic: head-to-head comparison of phosphorylated tau immunoassays. *Alzheimers Dement* **19**, 1913–1924.
72 Smirnov DS, Ashton NJ, Blennow K, Zetterberg H, Simrén J, Lantero-Rodriguez J, Karikari TK, Hiniker A, Rissman RA, Salmon DP *et al.* (2022) Plasma biomarkers for Alzheimer's disease in relation to neuropathology and cognitive change. *Acta Neuropathol* **143**, 487–503.
73 Barthélemy NR, Horie K, Sato C and Bateman RJ (2020) Blood plasma phosphorylated-tau isoforms track CNS change in Alzheimer's disease. *J Exp Med* **217**, e20200861.
74 Lantero-Rodriguez J, Snellman A, Benedet AL, Milà-Alomà M, Camporesi E, Montoliu-Gaya L, Ashton NJ, Vrillon A, Karikari TK, Gispert JD *et al.* (2021) P-tau235: a novel biomarker for staging preclinical Alzheimer's disease. *EMBO Mol Med* **13**, e15098.
75 Gonzalez-Ortiz F, Turton M, Kac PR, Smirnov D, Premi E, Ghidoni R, Benussi L, Cantoni V, Saraceno C, Rivolta J *et al.* (2023) Brain-derived tau: a novel blood-based biomarker for Alzheimer's disease-type neurodegeneration. *Brain* **146**, 1152–1165.
76 Cicognola C, Brinkmalm G, Wahlgren J, Portelius E, Gobom J, Cullen NC, Hansson O, Parnetti L, Constantinescu R, Wildsmith K *et al.* (2019) Novel tau fragments in cerebrospinal fluid: relation to tangle pathology and cognitive decline in Alzheimer's disease. *Acta Neuropathol* **137**, 279–296.
77 Mengel D, Janelidze S, Glynn RJ, Liu W, Hansson O and Walsh DM (2020) Plasma NT1 tau is a specific and early marker of Alzheimer's disease. *Ann Neurol* **88**, 878–892.
78 Chhatwal JP, Schultz AP, Dang Y, Ostaszewski B, Liu L, Yang HS, Johnson KA, Sperling RA and Selkoe DJ (2020) Plasma N-terminal tau fragment levels predict future cognitive decline and neurodegeneration in healthy elderly individuals. *Nat Commun* **11**, 6024.
79 Snellman A, Lantero-Rodriguez J, Emeršič A, Vrillon A, Karikari TK, Ashton NJ, Gregorič Kramberger M, Enik S, Paquet C, Rot U *et al.* (2022) N-terminal and mid-region tau fragments as fluid biomarkers in neurological diseases. *Brain* **145**, 2834–2848.
80 Chen Z, Mengel D, Keshavan A, Rissman RA, Billinton A, Perkinton M, Percival-Alwyn J, Schultz A, Properzi M, Johnson K *et al.* (2019) Learnings about the complexity of extracellular tau aid development of a blood-based screen for Alzheimer's disease. *Alzheimers Dement* **15**, 487–496.
81 Horie K, Barthelemy NR, Sato C and Bateman RJ (2021) CSF tau microtubule binding region identifies tau tangle and clinical stages of Alzheimer's disease. *Brain* **144**, 515–527.
82 Horie K, Li Y, Barthélemy NR, Gordon B, Hassenstab J, Benzinger TLS, Fagan AM, Morris JC, Karch CM, Xiong C *et al.* (2023) Change in cerebrospinal fluid tau microtubule binding region detects symptom onset, cognitive decline, tangles, and atrophy in dominantly inherited Alzheimer's disease. *Ann Neurol* **93**, 1158–1172.
83 Salvadó G, Ossenkoppele R, Ashton NJ, Beach TG, Serrano GE, Reiman EM, Zetterberg H, Mattsson-Carlgren N, Janelidze S, Blennow K *et al.* (2023) Specific associations between plasma biomarkers and postmortem amyloid plaque and tau tangle loads. *EMBO Mol Med* **15**, e17123.
84 Therriault J, Vermeiren M, Servaes S, Tissot C, Ashton NJ, Benedet AL, Karikari TK, Lantero-Rodriguez J, Brum WS, Lussier FZ *et al.* (2023) Association of Phosphorylated tau Biomarkers with Amyloid Positron Emission Tomography vs tau positron emission tomography. *JAMA Neurol* **80**, 188–199.
85 Grothe MJ, Moscoso A, Ashton NJ, Karikari TK, Lantero-Rodriguez J, Snellman A, Zetterberg H, Blennow K and Schöll M (2021) Associations of fully automated CSF and novel plasma biomarkers with Alzheimer disease neuropathology at autopsy. *Neurology* **97**, e1229–e1242.
86 Murray ME, Moloney CM, Kouri N, Syrjanen JA, Matchett BJ, Rothberg DM, Tranovich JF, Sirmans TNH, Wiste HJ, Boon BDC *et al.* (2022) Global neuropathologic severity of Alzheimer's disease and locus coeruleus vulnerability influences plasma phosphorylated tau levels. *Mol Neurodegener* **17**, 85.
87 Sato H, Kasuga K, Isoo N, Hayashi T, Ikeuchi T, Hori Y and Tomita T (2023) Soluble form of the APP fragment, sAPPβ, positively regulates tau secretion. *Neurosci Res* **193**, 63–70.
88 Sadleir KR, Kandalepas PC, Buggia-Prévot V, Nicholson DA, Thinakaran G and Vassar R (2016)

Presynaptic dystrophic neurites surrounding amyloid plaques are sites of microtubule disruption, BACE1 elevation, and increased Aβ generation in Alzheimer's disease. *Acta Neuropathol* **132**, 235–256.
89 Cassinelli Petersen G, Roytman M, Chiang GC, Li Y, Gordon ML and Franceschi AM (2022) Overview of tau PET molecular imaging. *Curr Opin Neurol* **35**, 230–239.
90 Kallinen A and Kassiou M (2022) Tracer development for PET imaging of proteinopathies. *Nucl Med Biol* **114–115**, 115–127.
91 Van Wambeke É, Gérard T, Lhommel R and Hanseeuw B (2022) Disclosing tau tangles using PET imaging: a pharmacological review of the radiotracers available in 2021. *Acta Neurol Belg* **122**, 263–272.
92 Tagai K, Ono M, Kubota M, Kitamura S, Takahata K, Seki C, Takado Y, Shinotoh H, Sano Y, Yamamoto Y *et al.* (2021) High-contrast In vivo imaging of tau pathologies in Alzheimer's and non-Alzheimer's disease Tauopathies. *Neuron* **109**, 42–58.e8.
93 Tezuka T, Takahata K, Seki M, Tabuchi H, Momota Y, Shiraiwa M, Suzuki N, Morimoto A, Nakahara T, Iwabuchi Y *et al.* (2021) Evaluation of [18F]PI-2620, a second-generation selective tau tracer, for assessing four-repeat tauopathies. *Brain Commun* **3**, fcab190.
94 Yap SY, Frias B, Wren MC, Schöll M, Fox NC, Årstad E, Lashley T and Sander K (2021) Discriminatory ability of next-generation tau PET tracers for Alzheimer's disease. *Brain* **144**, 2284–2290.
95 Brendel M, Barthel H, Van Eimeren T, Marek K, Beyer L, Song M, Palleis C, Gehmeyr M, Fietzek U, Respondek G *et al.* (2020) Assessment of 18F-PI-2620 as a biomarker in progressive Supranuclear palsy. *JAMA Neurol* **77**, 1408–1419.
96 Palleis C, Brendel M, Finze A, Weidinger E, Bötzel K, Danek A, Beyer L, Nitschmann A, Kern M, Biechele G *et al.* (2021) Cortical [18 F]PI-2620 binding differentiates Corticobasal syndrome subtypes. *Mov Disord* **36**, 2104–2115.
97 Kimura T, Ono M, Seki C, Sampei K, Shimojo M, Kawamura K, Zhang MR, Sahara N, Takado Y and Higuchi M (2022) A quantitative in vivo imaging platform for tracking pathological tau depositions and resultant neuronal death in a mouse model. *Eur J Nucl Med Mol Imaging* **49**, 4298–4311.
98 Vogel JW, Young AL, Oxtoby NP, Smith R, Ossenkoppele R, Strandberg OT, La Joie R, Aksman LM, Grothe MJ, Iturria-Medina Y *et al.* (2021) Four distinct trajectories of tau deposition identified in Alzheimer's disease. *Nat Med* **27**, 871–881.
99 Künze G, Kümpfel R, Rullmann M, Barthel H, Brendel M, Patt M and Sabri O (2022) Molecular simulations reveal distinct energetic and kinetic binding properties of [18F]PI-2620 on tau filaments from 3R/4R and 4R Tauopathies. *ACS Chem Nerosci* **13**, 2222–2234.
100 Kuang G, Murugan NA, Zhou Y, Nordberg A and Ågren H (2020) Computational insight into the binding profile of the second-generation PET tracer PI2620 with tau fibrils. *ACS Chem Nerosci* **11**, 900–908.
101 Murugan NA, Nordberg A and Ågren H (2021) Cryptic sites in tau fibrils explain the preferential binding of the AV-1451 PET tracer toward Alzheimer's Tauopathy. *ACS Chem Nerosci* **12**, 2437–2447.
102 Mishra SK, Yamaguchi Y, Higuchi M and Sahara N (2020) Pick's tau fibril shows multiple distinct PET probe binding sites: insights from computational modelling. *Int J Mol Sci* **22**, 1–15.
103 Murugan NA, Nordberg A and Ågren H (2018) Different positron emission tomography tau tracers bind to multiple binding sites on the tau fibril: insight from computational modeling. *ACS Chem Nerosci* **9**, 1757–1767.
104 Goedert M, Yamaguchi Y, Mishra SK, Higuchi M and Sahara N (2018) Tau filaments and the development of positron emission tomography tracers. *Front Neurol* **9**, 70.